

# ORBITERS, CUBESATS, AND RADIO TELESCOPES, OH MY; ENTRY, DESCENT, AND LANDING COMMUNICATIONS FOR THE 2018 INSIGHT MARS LANDER MISSION

Mark S Wallace\*, Daniel Litton†, Tomas Martin-Mur‡, Sean Wagner§

The Interior Exploration using Seismic Investigations, Geodesy, and Heat Transport (InSight) Mars lander mission was launched on May 5<sup>th</sup>, 2018 and its November 26, 2018 entry, descent, and landing sequence was observed by no less than five separate assets. The Mars Reconnaissance Orbiter (MRO) in orbit about Mars, the two Mars Cube One (MarCO) probes flying by, and two radio telescopes back on Earth were all used for this critical event communication coverage. These many paths of communication were enabled via the InSight launch/arrival strategy design, MRO orbital phasing selection, and MarCO trajectory design.

## INTRODUCTION

The Interior Exploration using Seismic Investigations, Geodesy, and Heat Transport (InSight) Mars lander mission, like the 2003 Mars Exploration Rovers<sup>1</sup> (MER), the 2007 Mars Phoenix Lander<sup>2</sup>, and the 2011 Mars Science Laboratory<sup>3</sup> (MSL) was required to have a communication path from the spacecraft back to Earth during the Entry, Descent, and Landing (EDL) sequence. The data thus returned are intended to aid in the reconstruction of any anomaly that should befall the spacecraft during EDL. These data would be invaluable to the resulting investigation and would aid future missions in avoiding the same fate. In addition, there is a strong desire for near-real-time assessment of the progress of EDL. Though the one-way light time is greater than the duration of EDL and thus no intervention would be possible, there is a very human desire to know how our robotic proxy is doing as quickly as possible. Having multiple assets in place, as well, provides redundancy in the event one or more assets are unavailable for any reason.

The InSight lander, being a near-clone of the Phoenix mission, could only communicate via UHF once the cruise stage is jettisoned before entry interface. This means that telemetry is only available via a proximity link. At the time of the design, the only assets available were the Mars Reconnaissance Orbiter (MRO), the Mars Atmospheric and Volatile Evolution (MAVEN) or the 2001 Mars Odyssey orbiters. ESA's Trace Gas Orbiter (TGO) had launched but had not yet entered orbit, while ESA's Mars Express (MEX) had an incompatible radio. MEX could detect a signal, but could not decode the telemetry. Similarly, UHF antennas on Earth could potentially detect a

---

\* Mission Design Engineer, Mission Design and Navigation Section, Jet Propulsion Laboratory, California Institute of Technology, Pasadena CA MS 264-820.

† Aerospace Engineer, NASA Langley Research Center, Hampton, VA MS 489

‡ Navigation Engineer, Mission Design and Navigation Section, Jet Propulsion Laboratory, California Institute of Technology, Pasadena, CA MS 264-820.

§ Navigation Engineer, Mission Design and Navigation Section, Jet Propulsion Laboratory, California Institute of Technology, Pasadena, CA MS 230-205.

signal, but the received power would be too low to decode the telemetry. This carrier-only signal would be of limited use in the event of an anomaly. At best, the presence or absence of a signal and its Doppler shift in the signal could say what was happening but not why. However, these ground-based assets would provide the best real-time indicators of the status of the spacecraft.

The Mars Cube One (MarCO) probes, being experimental cubesats, were not in the baseline for meeting this critical-event communication requirement. However, they did offer an opportunity to provide near-real-time telemetry to the ground. The MarCO probes were designed to provide a bent-pipe link and the near-real-time performance of the InSight EDL sequence. MRO could not provide that service, and the InSight launch/arrival strategy precluded using Odyssey, which could perform bentpipe relay, as it did for MSL. If the MarCO probes were successfully able to provide a real-time link, then future missions may be able to incorporate MarCO-class cubesats into their designs and free their launch/arrival strategies from being driven by critical-event communications requirements.

Once the launch/arrival strategy was selected and the MarCO probes were added to the launch manifest, the MRO phasing had to be selected and the MarCO flybys had to be designed. These designs were then validated via Monte Carlo analysis of the InSight EDL trajectories.

## ENTRY, DESCENT, AND LANDING OVERVIEW

From an EDL Communications perspective, the EDL sequence begins when the cruise stage is jettisoned 7 minutes prior to entry interface. When the cruise-stage is jettisoned, the X-band link to Earth is lost as the only antenna on the backshell is the UHF wrap-around antenna (WPA). Thirty seconds later, the aeroshell turns to the entry attitude. The spacecraft begins transmitting telemetry on UHF two minutes prior to entry and continues on the WPA UHF through parachute deploy, heatshield separation, and lander leg deployment. Communications switch to a helix UHF antenna mounted on the deck when the lander separates from the heatshield. This antenna is then used through touchdown and for the duration of the surface mission. See Figure 1.

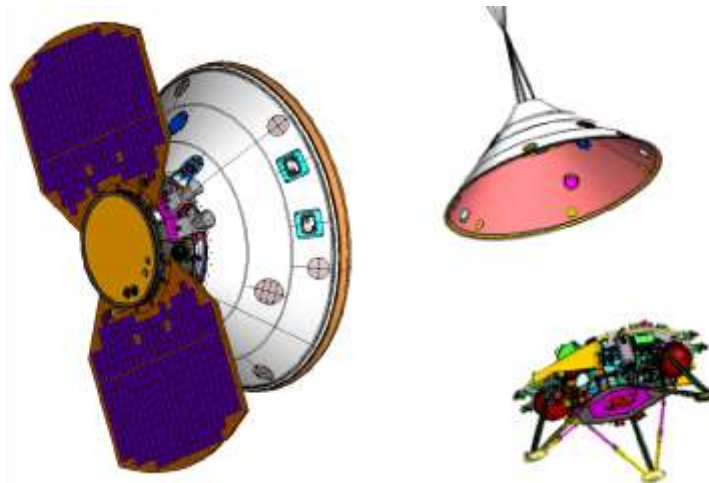


**Figure 1: InSight before entry (left) and just after lander separation (right).**

The backshell is a 45-deg half-cone and the WPA has much higher gains up to a field of view of 135 degrees relative to the point of the backshell, or put more simply, can see everywhere except “through” the heatshield. The large blue-and-green low-gain region of the WPA antenna pattern of Figure 2 illustrates this. In addition to this large obvious “null” are two other regions of concern. The first, in the center, is the null created by the parachute canister. This was referred to as the

“chute-can” null. The second is a trio of lows at about 45 deg off the point of the shell created by the edges of the three-panel WPA. One of these nulls is deeper than the others and is created by a slight mismatch between two of the panels. This is referred to as the “mismatch” or “WPA” null. All three of these nulls had to be considered during the design of the InSight and MarCO missions.

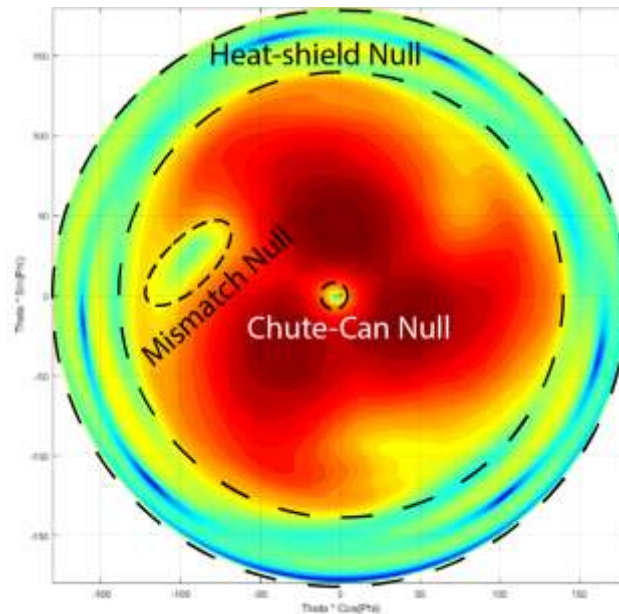


**Figure 2: Wrap-Around Antenna pattern with nulls annotated**

## LAUNCH AND ARRIVAL STRATEGY

As is traditional, the launch and arrival strategy was developed using a patched-conic analysis to determine the departure and arrival energies and geometries. These were synthesized in the also traditional “pork-chop plot,” illustrated in Figure 3. The primary non-EDL communications design constraint for the launch/arrival strategy was that the entry speed be less than 6.31 km/s, corresponding, for a prograde entry, to a velocity of hyperbolic approach (VHP) of 3.94 km/s, depicted as a thick red line. Launch declination (thick dashed green) and launch energy (thick blue) constraints also existed, but excluded only portions of the launch/arrival space. EDL communications ended up driving the launch/arrival strategy, shown as shaded regions.

The shaded regions are those where an orbiter has a phasing window at least 5 degrees of mean anomaly wide or the Earth’s position met the following geometric guidelines. First, the asset (orbiter or the earth) could be at least 10 degrees above the horizon at InSight touchdown through touchdown + 60 seconds and within the WPA field of view at entry interface. The field of view was assumed to be the entire sky except for the heat-shield null and thus the asset had to be within 135 degrees of the point of the backshell (also known as the “antenna angle”). The entry vehicle had a nominal 0 deg angle of attack and so this “boresight” was thus assumed to be the atmosphere-relative anti-velocity vector. Later comparisons between 3-degree-of-freedom and 6-degree-of-freedom EDL simulations confirmed this assumption. It was assumed that if such a line of sight exists at both entry interface and landing, the entirety of EDL would be similarly visible<sup>4</sup>. Monte Carlo simulation (see below) also confirmed this assumption. The elevation mask requirement for DTE was waived for launches between May 23<sup>rd</sup> and June 4<sup>th</sup>. The probability of launching in those days was low, the violation was small, and a 10 deg elevation mask is a standard mask to account

for multi-path effects off the surface; with no telemetry detectable on the DTE link, the very small violation was less of a concern.

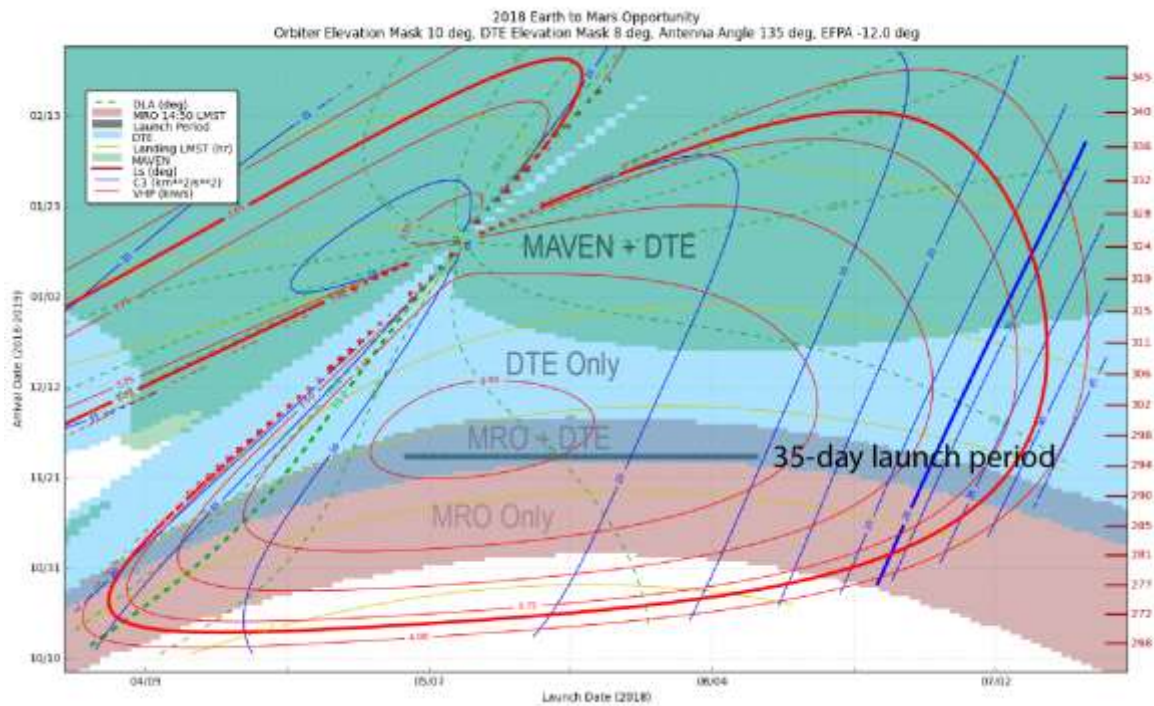


**Figure 3: Pork-Chop Plot illustrating EDL communications asset availability**

The selected launch/arrival strategy lay in the overlap of the MRO-visible region and the DTE-visible region. For a constant-arrival date strategy, there was an 11-day span of potential arrival dates with at least a 20-day launch period: November 25<sup>th</sup> to December 5<sup>th</sup>, 2018. The later the arrival date, the higher Earth would be in the sky at landing, but the further from MRO's ground-track the landing would be. The decision was made for a 35-day launch period extending May 5<sup>th</sup> to June 8<sup>th</sup>, 2018 with a constant arrival date on November 26<sup>th</sup>, 2018 to maximize the MRO capability without driving DTE right to edge of its capability. The geometries of the DTE and MRO links are tabulated in Tables 1 and 2, respectively.

The MAVEN coverage was discounted for two reasons: first, at the time of the design, the future MAVEN orbit was relatively uncertain. The duration of future deep-dip campaigns could dramatically alter the orbit's orientation due to their effect on nodal precession and apsidal rotation rates. The second reason is that most of the coverage depicted in Figure 3 was due to MAVEN being near its apoapsis during InSight's EDL, and there were concerns about the link performance at such relatively longer ranges.

**Table 1: Direct-to-Earth Geometries as a function of launch date**

Launch Date, 2018	Entry Time (11/26/2018, UTC)	Antenna Angle at Entry (deg)	Elevation at Landing (deg)	Elevation at Landing + 60 sec (deg)	Time to 0 deg Elevation (minutes)
May 5	19:39	20.2	14.5	14.2	65.9
May 6	19:41	20.3	14.0	13.8	64.0
May 7	19:43	20.4	13.6	13.4	62.1
May 8	19:45	20.5	13.3	13.0	60.4
May 9	19:46	20.6	12.9	12.7	58.8
May 10	19:48	20.7	12.6	12.4	57.3
May 11	19:49	20.9	12.3	12.1	56.0
May 12	19:50	21.0	12.0	11.8	54.7
May 13	19:52	21.2	11.7	11.5	53.5
May 14	19:53	21.3	11.5	11.3	52.4
May 15	19:54	21.5	11.3	11.1	51.4
May 16	19:55	21.6	11.1	10.9	50.4
May 17	19:56	21.8	10.9	10.7	49.6
May 18	19:56	22.0	10.7	10.5	48.8
May 19	19:57	22.1	10.6	10.4	48.1
May 20	19:58	22.3	10.4	10.2	47.5
May 21	19:58	22.5	10.3	10.1	46.9
May 22	19:59	22.7	10.2	10.0	46.5
May 23	19:59	22.8	10.1	9.9	46.1
May 24	19:59	23.0	10.1	9.8	45.7
May 25	20:00	23.2	10.0	9.8	45.5
May 26	20:00	23.4	9.9	9.7	45.3
May 27	20:00	23.6	9.9	9.7	45.0
May 28	20:00	23.8	9.9	9.7	45.0
May 29	20:00	24.0	9.9	9.7	45.0
May 30	20:00	24.2	9.9	9.7	45.1
May 31	20:00	24.3	9.9	9.7	45.2
Jun 1	20:00	24.5	10.0	9.7	45.3
Jun 2	20:00	24.7	10.0	9.8	45.5
Jun 3	19:59	24.9	10.1	9.8	45.8
Jun 4	19:59	25.2	10.1	9.9	46.1
Jun 5	19:59	25.4	10.2	10.0	46.5
Jun 6	19:58	25.6	10.3	10.1	47.0
Jun 7	19:58	25.8	10.4	10.2	47.5
Jun 8	19:57	26.0	10.6	10.3	48.1

**Table 2: MRO Geometries as a function of launch date (phasing window middle)**

Launch Date, 2018	Window Size (deg)	Antenna Angle at Entry (deg)	Elevation at Landing (deg)	Elevation at Landing + 60 sec (deg)	Time to 0 deg Elevation (minutes)
May 5	14.4	123.9	19.5	21.2	7.5
May 6	14.7	123.8	20.8	22.6	7.5
May 7	14.9	123.6	21.9	24.1	7.6
May 8	15.1	123.5	23.2	25.6	7.7
May 9	15.3	123.4	24.4	27.0	7.7
May 10	15.5	123.3	25.6	28.4	7.7
May 11	15.7	123.2	26.7	29.9	7.8
May 12	15.8	123.2	27.9	31.3	7.8
May 13	16.0	123.1	29.0	32.6	7.8
May 14	16.1	123.0	29.9	34.0	7.8
May 15	16.2	123.0	31.1	35.3	7.8
May 16	16.3	123.0	32.1	36.5	7.8
May 17	16.4	123.0	33.0	37.7	7.9
May 18	16.5	123.0	33.8	38.8	7.9
May 19	16.5	123.0	34.5	39.9	7.9
May 20	16.5	123.0	35.5	40.8	7.9
May 21	16.5	123.1	36.1	41.6	7.9
May 22	16.5	123.1	36.7	42.4	7.9
May 23	16.5	123.2	37.2	43.1	7.9
May 24	16.5	123.3	37.6	43.7	7.9
May 25	16.4	123.4	37.7	44.2	7.9
May 26	16.3	123.5	38.1	44.5	7.9
May 27	16.2	123.6	38.5	44.9	7.9
May 28	16.1	123.7	38.2	44.9	7.9
May 29	16.0	123.9	38.3	45.0	7.9
May 30	15.8	124.0	38.0	44.9	7.9
May 31	15.7	124.2	37.9	44.7	7.9
Jun 1	15.5	124.4	37.8	44.5	7.9
Jun 2	15.3	124.6	37.3	44.2	7.9
Jun 3	15.0	124.8	36.9	43.7	7.9
Jun 4	14.8	125.0	36.4	43.2	7.9
Jun 5	14.5	125.3	36.0	42.5	7.9
Jun 6	14.2	125.5	35.1	41.8	8.0
Jun 7	13.9	125.8	34.8	41.0	7.9
Jun 8	13.6	126.1	33.7	40.1	8.0

Between 19:39 and 20:00 UTC on November 26, 2018, the sub-Mars point on Earth was 10.2 deg South latitude and between 21.5 and 26.7 West longitude, 917 km (570 miles) off the coast of Recife, Brazil. As a result, radio telescopes in Western Europe and on the East coast of the US could potentially detect the UHF signal, as Mars would be above the horizon during EDL. See Figure 4. The radio telescopes at Green Bank in West Virginia and Effelsberg, Germany were configured to do so and communicate those results to mission control at JPL.

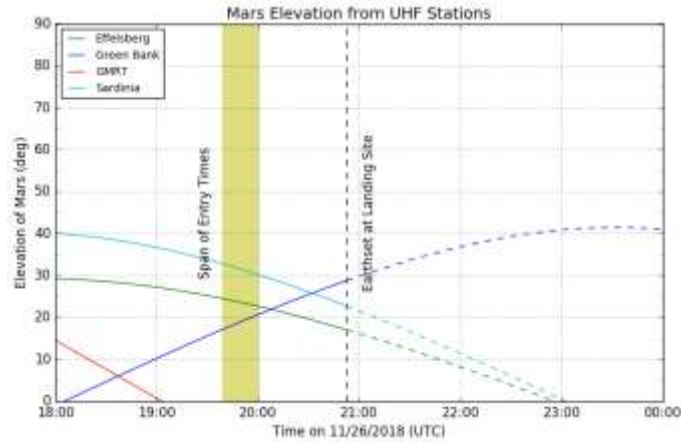


**Figure 4: Mars Elevation from Terrestrial UHF Stations**

The final design had the approach geometry described in Figure 5. MRO, in this figure, is phased to the middle of its window, and it, along with the other assets, are illustrated at the time of entry with the point of the arrows indicating their locations at landing, which is where the InSight trajectory ends. The other orbiters (Odyssey, MAVEN, and Mars Express) are unphased as none of them could be phased for even partial coverage of InSight's EDL.

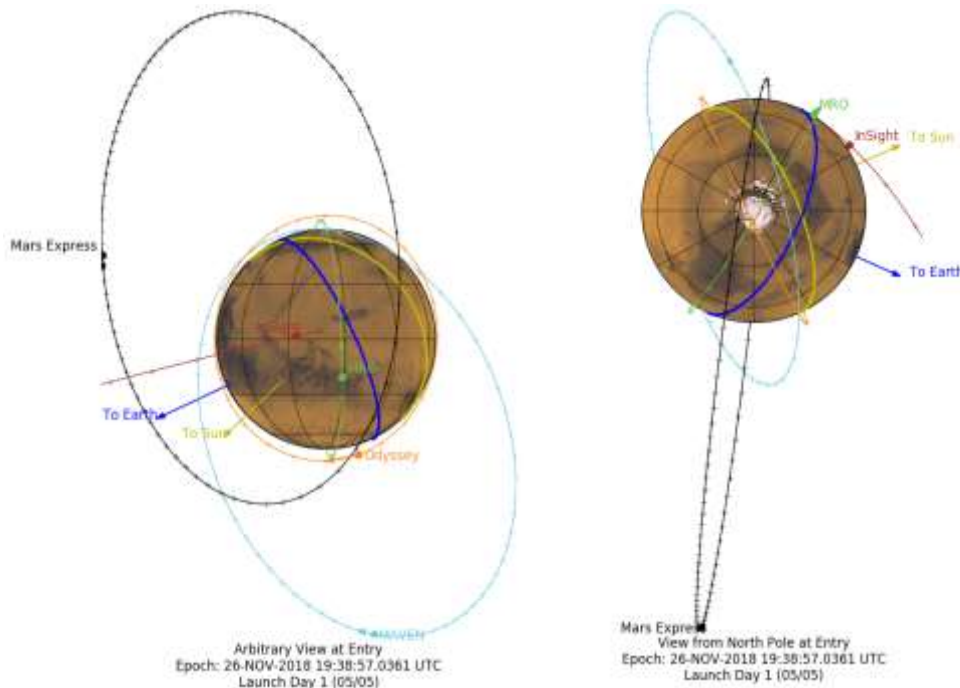


**Figure 5: Designed Arrival Geometry with in-situ orbiters**

## SELECTION OF MRO PHASING

The interface to MRO was the Entry Relay Target File, or ERTF, which specifies a latitude at which the InSight project requests that MRO achieve at its entry time. MRO committed to reaching that latitude within 30 seconds of the requested epoch. This was parameterized as the mean anomaly of MRO at the InSight entry time, and the 30 seconds was equivalent to 1.6 deg. At the open of the InSight launch period, the phasing window was 14.4 deg wide, and so the InSight project had a range of targets from which to choose. A “phasing map,” an example of which is illustrated in Figure 6, was used to visualize the trades involved.

The horizontal axis is time since entry and the vertical axis is a potential MRO mean anomaly at the entry epoch. Reading horizontally then is moving in time, while reading vertically is changing the phasing. The contours are the slant range. The colors mean different things before and after landing. Prior to landing, the white-colored regions are those where MRO is occulted by Mars, the red region is where a line of sight exists, but it is through the heat-shield null, and the green region is not. The yellow region is one where, if InSight is rolled just right, MRO could be within the mismatch null (called the WPA null in the legend). However, since the roll is uncontrolled during EDL prior to lander separation, it was believed that mismatch null passages would be brief. After landing, the colors indicate elevation ranges, as described in the legend.

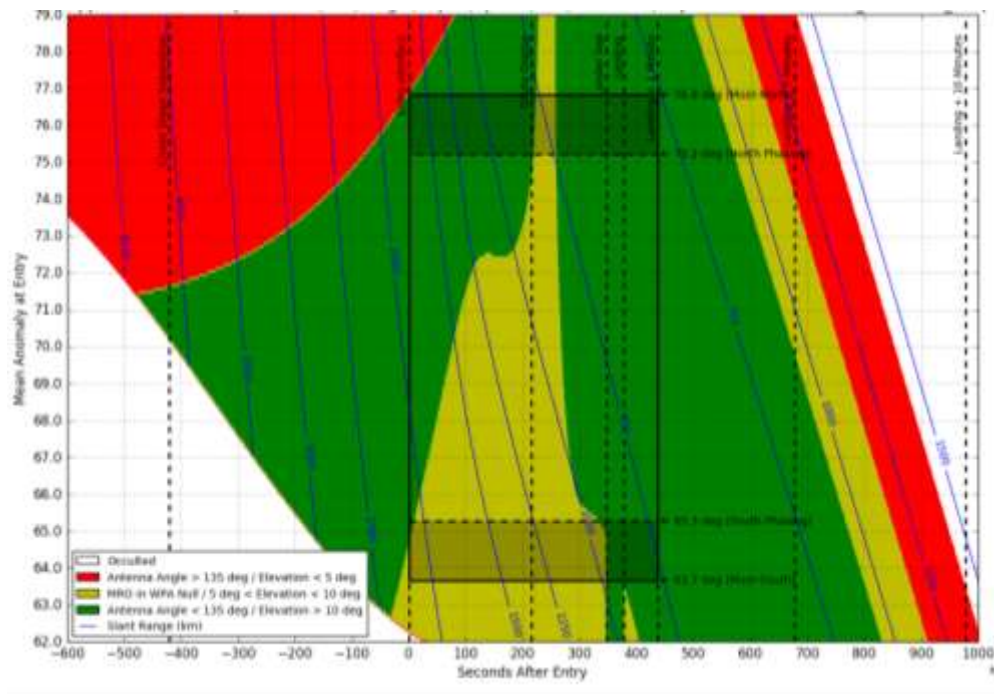


**Figure 6: MRO Phasing Map**

The solid black lines running horizontally at 76.8 and 63.7 deg mean anomaly indicate the furthest north and south MRO could be phased to and still meet the geometric guidelines. At 76.8 deg, MRO is coming out from behind the heat-shield at entry, while at 63.7 deg, MRO is only 10 deg above the horizon five minutes after landing. The shaded regions next to these lines denote the  $3\sigma$  bounds on MRO's targeting ability and thus show the furthest north (75.2 deg) and south (65.3 deg) a phasing target could be specified, assuming no dispersions within the InSight EDL trajectory.

Consider a phasing of 70 degrees; as seen from InSight, MRO comes out from behind the limb of Mars just after cruise stage separation at a range of about 4100 km. By entry, the range has

dropped below 2000 km and unfavorable roll angles could place MRO within the mismatch null between 100 and 250 seconds after entry. The MRO-InSight range is 750 km at lander separation. MRO is well above 10 deg elevation at landing and remains so through landing + 5 minutes.

As can be seen in this map, the shortest ranges occur when MRO is phased closer to the north edge of the window, while the longest post-landing contact duration occurs when MRO is phased closer to the south edge of the window. Monte Carlo analyses of the link budget, discussed below, confirmed that the link was ever so very slightly better with northern phasings and that the duration of the post-landing contact was indeed better with southern phasings. Further, southerly phasings spent more time in the mismatch null and had a higher risk of drop-outs during null transits. Since the requirements could be met nearly anywhere in the window, the decision was made for MRO to be targeted to the middle of the window to maximize the margins.

## **MARCO TRAJECTORY DESIGN**

The MarCO trajectory design was not nearly so simple as the MRO phasing decision. The MRO phasing problem is essentially one-dimensional - where is it alongtrack? The MarCO trajectory design was three-dimensional: a B-Plane target and time of closest approach. As a result, a more sophisticated approach was taken using a simplified link budget. The requirements for MarCO were to be able to relay the 8 kbps InSight UHF telemetry data from the time when transmission started, approximately two minutes before entry, to when it ended, five minutes after landing. It was also desired to acquire the UHF carrier when it started, seven minutes before entry. The MarCO probes did not carry enough propellant to enter into Mars orbit, so they performed a flyby of Mars as they were relaying the InSight data. That meant that their velocity relative to InSight was small during the approach, but grew as soon as InSight hit the atmosphere of Mars and was larger than MRO's relative velocity during final descent and when InSight was on the surface. We initially used just the nominal InSight trajectory in order to search for the optimal flyby conditions. We assumed that InSight's was oriented so the center of the parachute cone was pointing against the Mars-relative velocity, but did not make any assumption in clock angle, using in the initial analysis the 10% low value of the InSight antenna gain for the given cone angle. After parachute deploy and before lander separation, we also assumed wrist motion with up to 11° of amplitude, using the worst possible gain for cone angles in the wrist motion range with respect to the nominal cone angle. For evaluating the gain of the MarCO antenna pattern, we used the nominal position of InSight. With these assumptions, we calculated the minimum margin during the 8 kbps relay for a range of B-plane targets and periapsis times. The result was a map like the one shown in Figure 7, showing regions where the minimum margin was above some threshold for the optimal MarCO periapsis time, and also showing the optimal margins. The contours shown start at 3 dB of margin

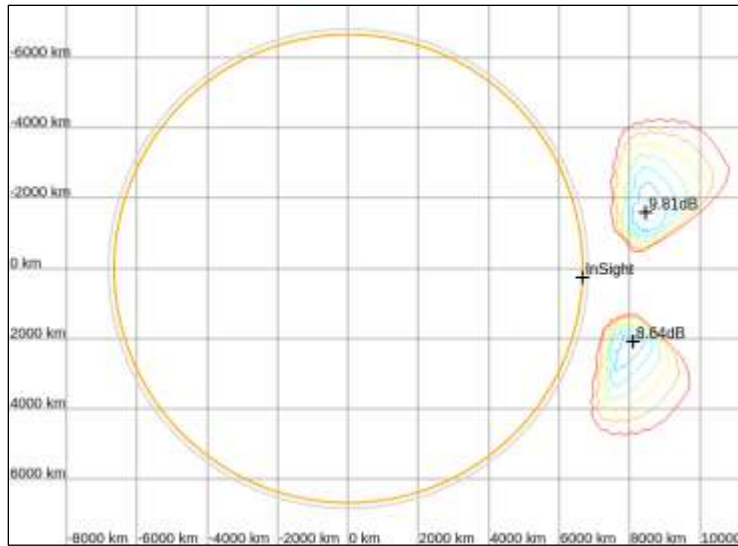


**Figure 7: MarCO 8 kbps UHF Relay Margin Contours**

Due to the chute-can null in the InSight antenna pattern, the contours split in two separate regions. That put the possible MarCO targets north and south of the incoming InSight orbit plane (see Figure 8) in order to avoid the null. If they had been in the same plane, then as InSight began its turn to vertical while under the chute, the chute-can null would have swept through the InSight-MarCO line of sight and disrupted the signal. By placing one MarCO in the northern target and the other at the southern target, the impact of the mismatch null could be minimized. If InSight were rolled such that this null was pointed at one MarCO, it could not simultaneously be pointed at the other.

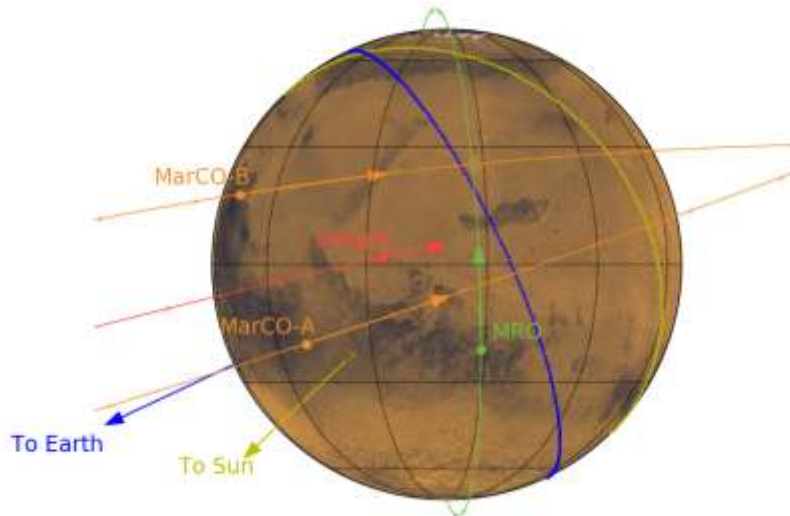


**Figure 8: MarCO Flyby and MRO Overflight**

For each point in those regions, the link geometry and performance was analyzed for different periapsis times. Figure 9 shows a sample of this evaluation. Part of the optimization was the selection of a MarCO attitude that would produce the highest UHF margin while keeping the MarCO HGA boresight pointed to the Earth. The position of Mars with respect to the MarCO star tracker field of view was also evaluated to ensure a stable attitude during relay.

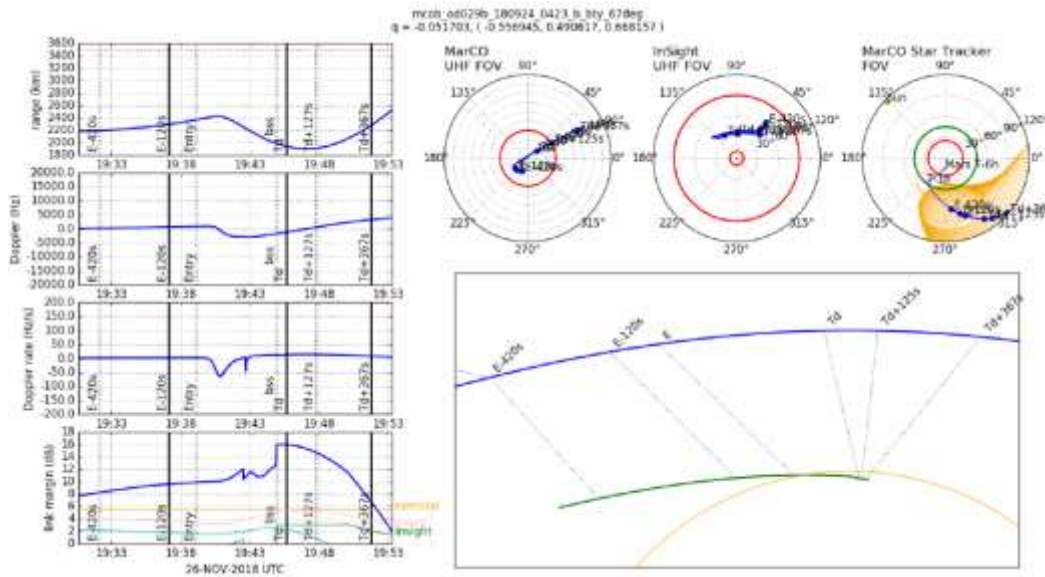


**Figure 9: Sample MarCO Relay Evaluation using InSight Nominal Trajectory**

## MONTE CARLO VALIDATION

The processes used to choose the MRO phasing and the MarCO flyby targets used a nominal InSight EDL trajectory. However, there are significant uncertainties in the EDL trajectory, and Monte Carlo analyses were undertaken to quantify the resulting variations in the link margins and the geometries.

### Models

POST2 is a 6 degree-of-freedom flight dynamics simulation used to model the entry, descent, and landing of InSight starting ten minutes prior to Mars atmospheric interface through five minutes after touchdown. POST2 pulls together models of atmosphere, aerodynamics, flight software, thrusters, mass properties, etc in order simulate the flight dynamics of a vehicle. POST2 takes all of the models and outputs the dynamic location and attitude of the vehicle through the whole trajectory. The software has been used for Mars Science Laboratory, Phoenix, Mars Exploration Rover, Mars Reconnaissance Orbiter, and Orion Launch Abort System among many other missions.

A communications module is included in POST2 that allows the calculation of link quality between two vehicles (transmitter of one and the receiver of the other). The communications module takes into account the antenna gain patterns on both vehicles, the orientation of both vehicles, space loss between the vehicles, transmitter and receiver powers, polarization loss, and circuit losses among other parameters. Figure 2 shows the InSight WPA, which is utilized up until the lander separates from the backshell. InSight then switched to the Helix antenna shown in Figure 10 (left) after the lander has separated. Finally, the MRO receiving antenna pattern is shown in Figure 10(right). The antenna pattern tells the quality of the signal coming out of that particular boresight location. Since POST2 outputs the dynamic location and attitude of the vehicle as it goes through the atmosphere, it enables a high fidelity calculation of the signal link quality from InSight to MRO, MarCO-A and B, and Earth-based assets.

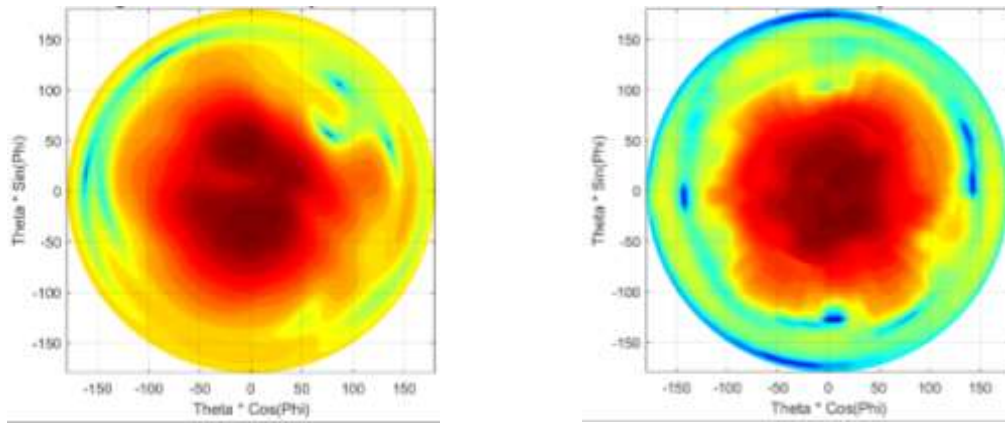


**Figure 10: InSight (left) and MRO (right) Helix antenna patterns**

Since there are uncertainties in the atmosphere, mass properties, aerodynamics, entry state, etc, Monte Carlo cases are used to understand the impact and range of different possible trajectories and attitudes InSight could possibly traverse. Different trajectories and vehicle attitudes can cause differences in the portions the antenna pattern will be looked through and space loss differences. It was determined that 900 different trajectories (each one a random draw on atmosphere, mass properties, aerodynamics, entry state, etc) were enough to cover the trade space and feel confident and have confidence in the accuracy in the results. Additionally, a “beard” (-5.3 dB under the WPA, and -3.7 dB under the Helix) was added to the one-percentile low to cover dispersions such as knowledge of the antenna gains and circuit losses from the WPA and Helix antennas.

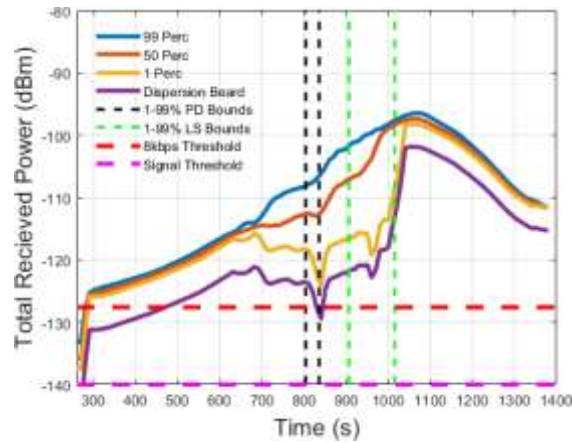
## Results

The Monte Carlos results were used to determine the MRO phasing choice, inform the slew designs to keep InSight in the MRO UHF antenna field-of-view while attempting to take a picture, and refine the MarCO trajectory design. They also informed MarCO trajectory correction maneuver go/no-go decisions. For each asset (MRO, MarCO-A, MarCO-B, Green Bank, and Effelsburg), a threshold was defined above which the signal strength would be sufficient to meet requirements. For MRO and the MarCOs, that was 8 kbps data rate. For the radio telescopes, that was unambiguous real-time signal detection. If the DTE signal was below the threshold, it would still be detectable if it were steady enough. In general, that meant the signal was only detectable pre-entry or post-landing. In addition to the link budget, each asset had to be above 10 deg elevation through one (MRO) or five (MarCO) minutes after touchdown.

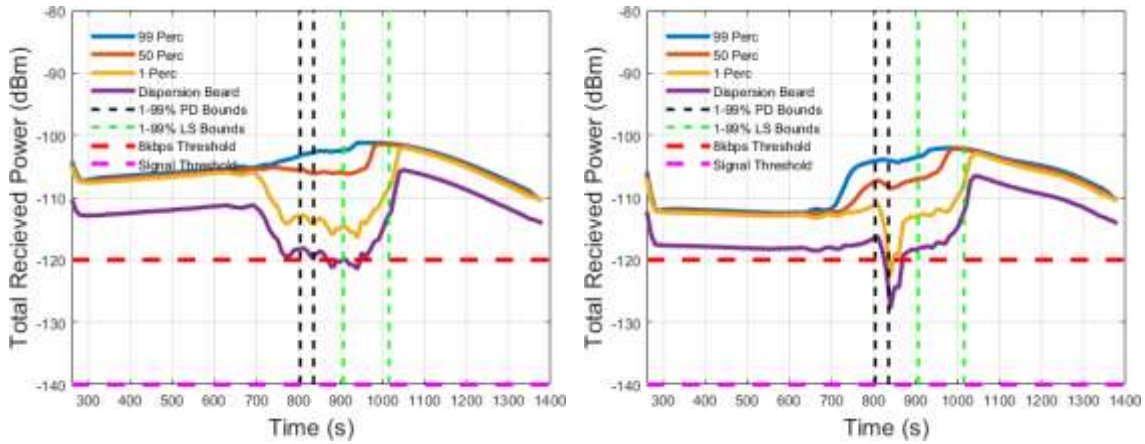
The primary method of assessing the link margin was to plot the received power vs. time, as in Figures 11 through 13. Each of these plots illustrates the 99<sup>th</sup>, 50<sup>th</sup>, and 1<sup>st</sup> percentile of minimum received power in the previous 10 seconds in the Monte Carlo at each time-step, with entry interface occurring at 600 seconds. Additionally, the purple line represents the worst case, the 1<sup>st</sup> percentile minus the beard described above. In each of the figures, the dashed lines indicate the 1<sup>st</sup> and 99<sup>th</sup> percentile time range for parachute deploy (PD, in black) and lander separation (LS, in green). Much of the large differences between the 1<sup>st</sup> and 99<sup>th</sup> percentile received power relative to the 50<sup>th</sup> percentile is due to the dynamics under the parachute causing the boresight to sweep through low gain areas in the WPA and Helix antenna patterns. Specifically, the mismatch and chute-can nulls cause the largest drop-outs while under the parachute.

Figure 10 shows that the link quality for MRO is above the threshold with margin, except for a short duration after parachute deploy. MarCO-A’s worst cases have a few poke outs below the threshold, but otherwise demonstrates good link quality. MarCO-B, on the other hand, has a large

poke-out around parachute deploy that is caused by MarCO-B being on the other side of InSight and therefore became more exposed to the WPA “mismatch” null. As was expected, the signal quality to Green Bank and Effelsberg is not great, mainly due to the distances between Earth and Mars. The dynamics of parachute deploy take Green Bank’s link quality below the threshold.



**Figure 11: MRO Received Power Plot**



**Figure 12: MarCO-A (left) and MarCO-B (right) Received Power Plots**

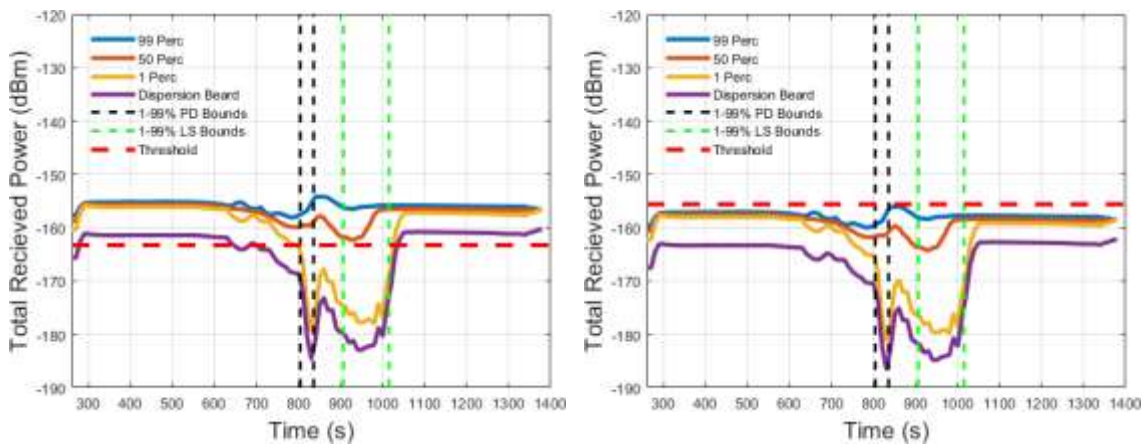


**Figure 13: Green Bank (left) and Effelsberg (right) Received Power Plots**

The second method of assessing performance was to tabulate the link margin and elevation at specific key points along the EDL trajectory, as in Table 3. The received power plots told an end-to-end story in time, but the metric tables captured the performance at discrete events that missed much of the larger drop-outs shown Figures 11 through 13. For example, the 1% low MRO link at chute deploy was 4.4 dBm above the threshold, while the power plot showed a small number of cases below it. The dynamics of and after chute deploy were the cause of the drop offs shown in Figures 11 through 13. The Project prioritized MRO and MarCO phasing and link quality between lander separation and touchdown. The metric tables gave a quick look into the signal quality where the received power plots quantified the whole link quality picture. The metric table was used to evaluate against the elevation requirements.

**Table 3: Example Link and Elevation Performance**

Metric	Units	Margin to Requirement: 1 <sup>st</sup> Percentile Monte Carlo minus “Beard”				
		MRO	MarCO-A	MarCO-B	Green Bank	Effelsberg
Link at Entry Interface	dBm	4.7	8.6	1.9	1.6	-8.0
Link at Chute Deploy	dBm	4.4	3.3	4.6	-3.8	-13.4
Link at Lander Separation	dBm	10.4	10.9	9.7	-11.7	-21.3
Link at Touchdown + 1 minute	dBm	25.3	13.6	12.3	2.5	-7.1
Link at Touchdown + 5 minute	dBm	N/A	6.7	6.9	2.2	-7.4
Minimum Elevation from Touchdown to Touchdown + 1 minute	deg	3.5	37.9	40.6	1.7	1.7
Minimum Elevation from Touchdown to Touchdown + 5 minute	deg	N/A	22.6	34.2	10.9	10.9

## IN FLIGHT: MRO

The phasing windows were found by taking a nominal MRO trajectory and shifting the mean anomaly while holding the rest of the mean (as opposed to osculating) elements constant. In this way, a new phasing could be evaluated quickly and without designing the phasing maneuver(s) necessary to achieve this new phasing. However, such maneuvers would need to be executed in reality, and this approximation thus introduces a small error. To eliminate this effect, an iterative process, illustrated in Figure 14, was undertaken on a monthly cadence post-launch. The MRO Navigation Team delivered a new trajectory each month in response to an ERTF and the InSight team undertook a set of Monte Carlo analyses with the latest InSight entry uncertainties, MRO slew designs, and the current  $1\sigma$  and  $3\sigma$  up-track and down-track uncertainties in the MRO position. This resulted in as many as five Monte Carlos being run for each cycle through this process. In every case, the performance was satisfactory and the phasing target was unchanged. The ERTFs were updated bi-weekly and after each TCM to track the changes in the InSight entry time, but the decision to target the middle of the phasing window was never changed. This same process was used to refine the MRO slew designs in the hopes of capturing a picture of InSight on the parachute with the HiRISE imager, but unfortunately, the picture was saturated.

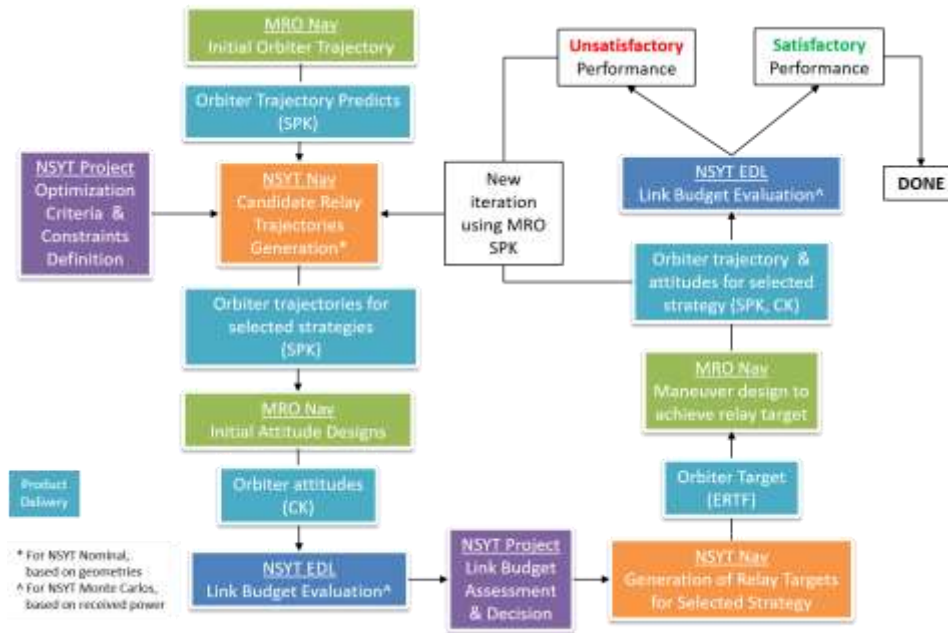


**Figure 14: MRO-InSight Iterative Process**

The evolution of the InSight entry time and resulting latitude target from pre-launch (ERTF-01) to the finalization of the phasing target (ERTF-15) and the final entry time predict prior to the execution of TCM-6 (ERTF-20) is illustrated in Figure 15. The major shifts in entry time are due execution errors along the trajectory, post-launch updates to the EDL trajectory tools, and an update to the landing site target to optimize landing site safety for the specific approach azimuth. Execution errors in the launch and the earlier, larger TCMs (particularly TCM-1 and TCM-2) affected the approach v-infinity vector enough to shift the entry point required to meet the landing site. The small shifts are due to execution errors in TCM-4 and ongoing changes in the prediction due to the orbit determination uncertainty.

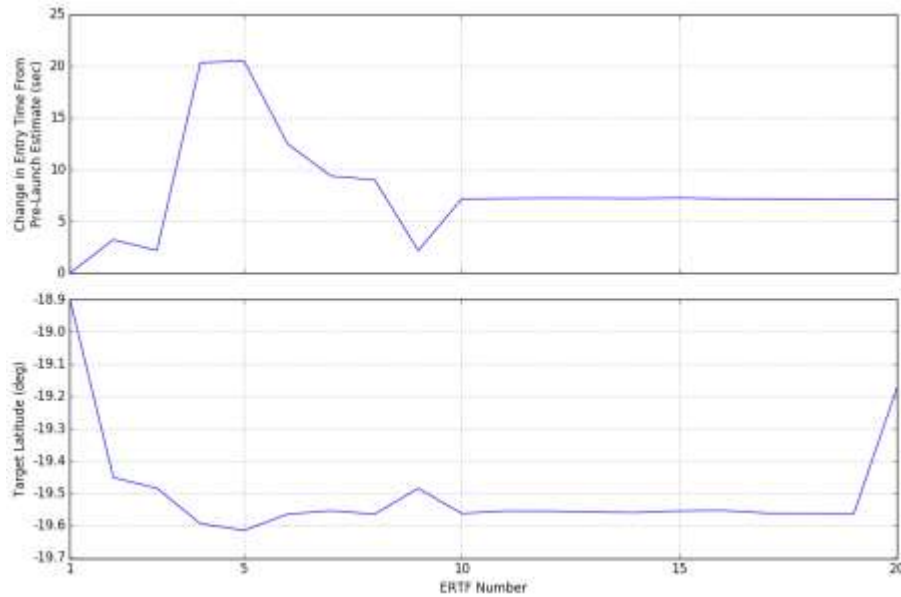


**Figure 15: Entry Time and MRO Target Latitude Evolution**

The latitude shift for ERTF-20 requires some discussion. That ERTF was unique in that the InSight trajectory used to assess the MRO phasing window included a TCM design based on one orbit determination solution but an initial state based on a solution generated a few days later. The shift from one solution to the other was very small – less than  $1\sigma$ , but the effect was for the spacecraft to land slightly south and a little west of the target. As the effective target was to the west of the MRO ground-track (see Figure 8), this offset meant MRO would be lower in the sky at landing for a fixed phasing. Further, since the south edge of the window was defined by the elevation at landing (see Figure 6), this offset shifted the south edge northward, which shifted the middle of the window north as well. The Monte Carlo analyses included the effect of an initial state error in the maneuver design as part of the entry state dispersions, and so this was, in effect, a partial collapse of the probability cloud. The InSight-MRO geometries did not suddenly change at ERTF-20.

The MRO Navigation strategy for phasing to the InSight EDL relay target is more thoroughly described elsewhere<sup>5</sup>, but in brief, the design was for two maneuvers with a third contingency maneuver, referred to as Orbit Synchronization Maneuvers (OSMs). The first maneuver, OTM-50 (OSM-1), was executed on August 22<sup>nd</sup> and reduced the phasing error by 42.7 minutes from 55.2 minutes to 12.5 minutes (to the anticipated  $3\sigma$  timing uncertainty) using the ERTF-10 target. The second maneuver, OTM-51 (OSM-2), was performed on October 24<sup>th</sup> to remove the remaining error relative to the ERTF-15 target. The third burn, OSM-3 scheduled for November 14<sup>th</sup>, was not necessary, as the predicted phasing error of  $-4.05 \pm 24.1$  seconds ( $3\sigma$ ) at the November 5<sup>th</sup> DCO was within the  $\pm 30$  second commitment to the ERTF-15 target. On November 12<sup>th</sup>, just a few days prior to the planned OSM-3, this phasing error further reduced to  $-8.7 \pm 10.9$  seconds ( $3\sigma$ ). This also eliminated the need for a contingency OSM-3 on November 19<sup>th</sup> since this phasing correction would be too small to perform. The final MRO trajectory reconstruction at the InSight EDL target was 8.4 seconds late to the ERTF-15 latitude (i.e. south of the target at the entry epoch).

## IN FLIGHT: MARCO

As the MarCO probes separated from the upper stage of the launch vehicle, their respective separation mechanisms pushed them into trajectories in both sides of the InSight trajectory. If left uncorrected, they would have passed tens of thousands of kilometers away from Mars. Within days of launch, it was apparent that MarCO-B suffered from an internal leak between the propellant tank and the plenum that allowed liquid to accumulate at the plenum. This condition had been already been seen during pre-launch testing, but it was accepted as it would not have been possible to fix the problem before the probe had to be delivered for integration into the launch vehicle. Sometime after, an external leak in one of the attitude-control thrusters also developed, creating a torque that pushed the spacecraft into frequent angular momentum reduction maneuvers. The leak and the maneuvers had a translational effect that perturbed the trajectory of the probe. A strategy was developed to reduce the amount of propellant in the plenum, and so keep it in a gaseous state, by performing frequent plenum blowdowns that further affected the trajectory. Meanwhile, thruster calibration burns were performed in MarCO-A to characterize its propulsion system. The first trajectory correction maneuver to bring MarCO-A closer to Mars was performed on May 22, 2018. For MarCO-B, after the leak mitigation measures were in place and a reliable trajectory determination could be performed, the first trajectory correction maneuver was executed on May 22, 2018. Further trajectory correction maneuvers (TCMs) were executed to bring both probes closer to their respective flyby targets, to compensate for the higher than usual—for deep-space probes—maneuver execution errors and, in the case of B, to compensate also for the effects of the propellant leaks.

The MarCO team leveraged the ERTF-Monte Carlo iterative process of Figure 14 as well. For each Monte Carlo analysis the InSight team undertook, the MarCO team provided a number of

additional potential MarCO trajectories for each spacecraft to explore the design space more thoroughly. These variations were initially designed to yield the partials of the link margin in each phase of EDL as a function of the MarCO flyby parameters and were then later used to balance the link margin across EDL at the 1<sup>st</sup> percentile rather than for the nominal. One change to the way the targets were selected came from the realization that the dispersion due to InSight's trajectory and attitude uncertainties were much larger during the parachute and divert phase than during the on-surface phase. A rebalancing of the margin across the relay was performed, aiming for higher margins during the most dynamic phases and smaller margins during the on-surface phase, shifting the flyby targets. Figure 16 illustrates the targeting challenge for the MarCO probes with one of the Monte Carlo samples. The relative trajectory and attitude motion between both spacecraft moved the position of the MarCO probes in the InSight antenna patterns, and the features in these patterns made accommodating this motion challenging.

After each TCM, the relay performance was reevaluated using the latest trajectory predicts to assess whether further TCMs were warranted. A plenum leak also surfaced on MarCO-A, making maneuver performance also less reliable for this probe, but since MarCO-A did not have an external leak, its trajectory was not continuously perturbed as it was for B. The last TCM for MarCO-A was executed on October 3, 2018, leaving the spacecraft 320 km away from its flyby B-plane target and one minute early in arrival time. The last TCM for MarCO-B was performed on November 16, 2018, leaving this probe in a trajectory 110 km away for its flyby B-plane target and 4 seconds early in arrival. The final targeting errors for both MarCO did not grant further TCMs, as the performance assessed using the Monte Carlo analysis was deemed to be within the expected link-budget uncertainty.

Both MarCOs performed very well during InSight's descent into Mars, relaying the InSight UHF data with only a short data loss during the plasma black out. The data relayed by the MarCO probes allowed the InSight team to assess the state of their spacecraft in near real time during EDL and also included a picture taken by InSight soon after it landed on the surface of Mars.

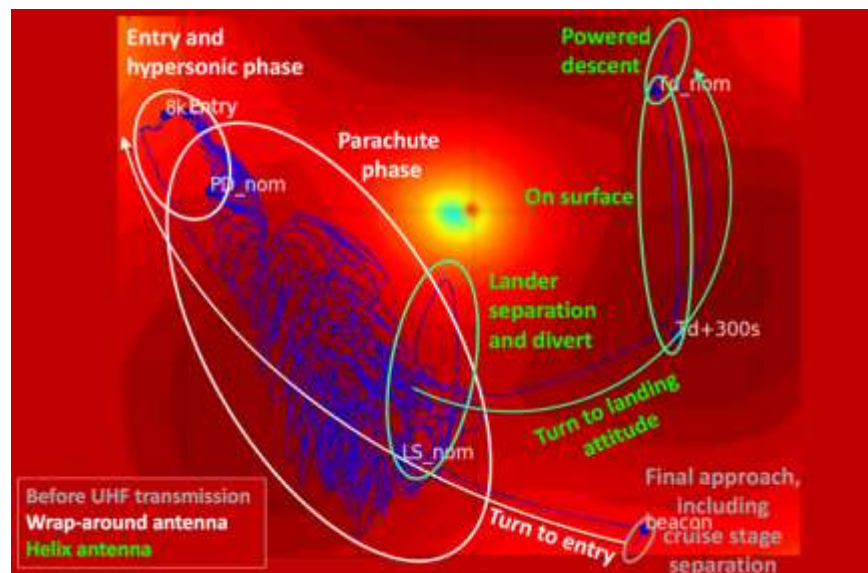


**Figure 16: Sample MarCO-B Path in the InSight WPA antenna pattern**

## IN FLIGHT: EARTH

The radio telescopes, once identified and configured, required a set of predicts for what signal to expect. The Doppler shift of InSight's UHF signal from entry to touchdown was dramatic. The net 6 kHz shift far exceeds what the radio telescopes could do without a predict. In particular, the parachute deployment was predicted to be nearly 200 Hz, and that would be swamped by the total shift. See the 100 cases of an example Monte Carlo in Figure 17 as compared to the nominal (in red). Differencing these 100 cases from the nominal yields the curves in Figure 18. There are two structures of note in this plot. The first is the variation as the peak-deceleration timing varies in the nominal and the second is the sharp jump at parachute deploy. This parachute deploy jump could be either positive or negative, or even non-existent, if the actual trajectory was very close to the nominal. There was concern that it would not necessarily be unambiguous when chute deploy occurred. The Doppler difference from a no-chute trajectory is illustrated in Figure 19. In this plot, the parachute deployment shows up as a minimum +200 Hz jump in the signal, no matter what the hypersonic phase encountered. The second jump is an artifact here, where the no-chute reference trajectory experiences a large instantaneous velocity change when it hits the ground at several hundred meters per second.

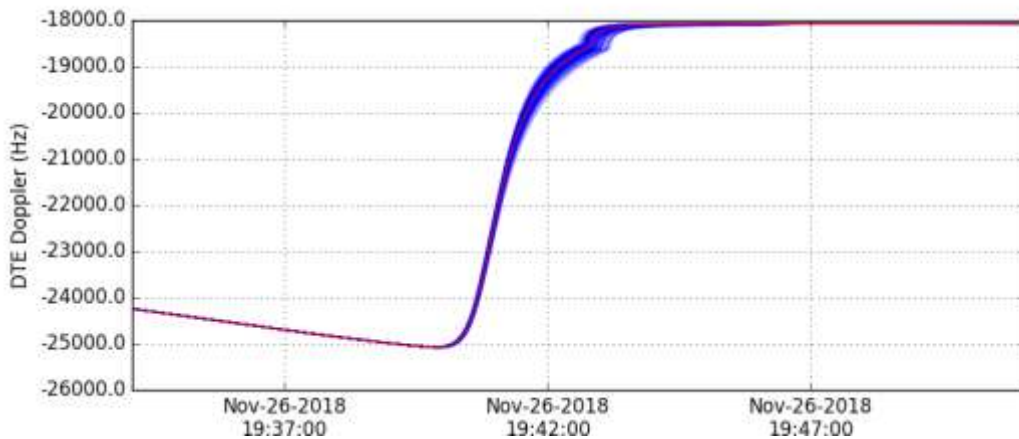


**Figure 17: DTE Doppler Shift, 100 Monte Carlo cases in Blue, Nominal in Red**

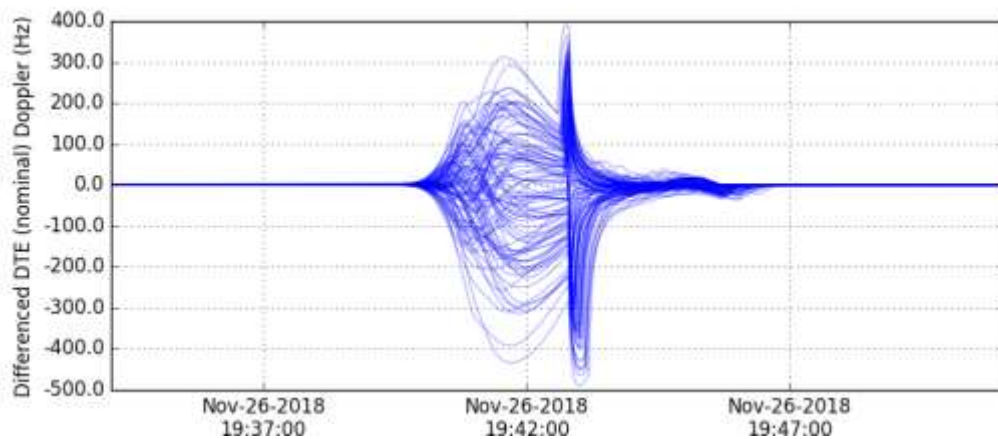


**Figure 18: DTE Doppler Difference from Nominal Trajectory (100-case Monte Carlo)**

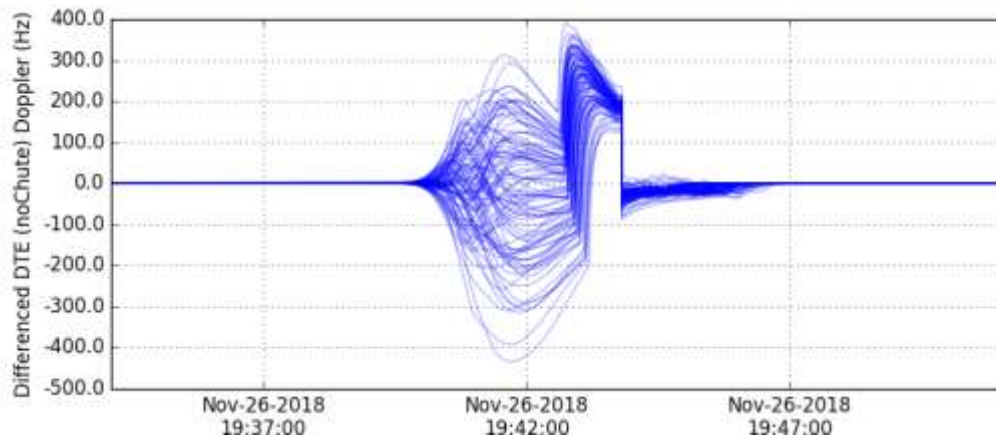


**Figure 19: DTE Doppler Difference from No-Chute Trajectory (100-case Monte Carlo)**

By using a no-chute trajectory as a reference, the radio science team could watch the power spectrum wander around a little bit during entry and know that a large and sudden positive shift would be parachute deploy. The sudden jump back toward zero shift would be discounted, and when it stopped shifting they would know the spacecraft had come to rest at the surface. The recorded Doppler shift during EDL is shown in Figure 20. The noisy features are, from left to right, prior to UHF turn on, the plasma blackout, and after the UHF was turned off five minutes after landing.

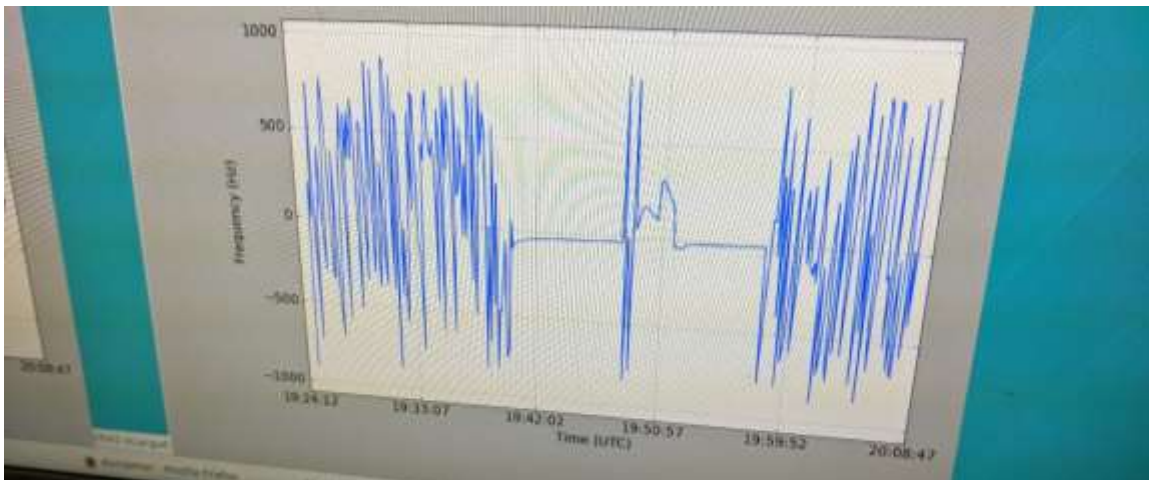


**Figure 20: Recorded Doppler Shift during EDL**

## CONCLUSION

On November 26<sup>th</sup>, 2018, at 10 am Pacific Standard Time, the InSight and MarCO teams gathered in their respective mission support areas in Pasadena and in Denver to await word that InSight had safely landed on the surface of Mars. The telemetry and Doppler shifts they used to inform themselves and the public what was happening 95 million miles away was available through the combined pathways of two CubeSats, an orbiter, and two radio telescopes, all of whom were focused on the “seven minutes of terror.”

## ACKNOWLEDGMENTS

The research described in this paper was carried out at the Jet Propulsion Laboratory, California Institute of Technology, under a contract with the National Aeronautics and Space Administration. The authors would like to acknowledge the members of the InSight, MRO, MarCO, and Radio Science Teams who contributed to the analyses that are reported on in this paper. © 2018 California Institute of Technology. Government sponsorship acknowledged.

## REFERENCES

- <sup>1</sup> Hurd, W.J., Estabrook, P. Racho, C.S. and Satorius, E.H. “Critical Spacecraft-to-Earth Communications for Mars Exploration Rover (MER) Entry, Descent, and Landing,” 2002 IEEE Aerospace Conference Proceedings, Vol 3. IEEE Publications, Piscataway, NJ, 2002, pp 1283-1292
- <sup>2</sup> Kornfield, R., Garcia, M., Craig, L., Butman, S., and Sinori G., “Entry, Descent, and Landing Communications for the 2007 Phoenix Lander,” *Journal of Spacecraft and Rockets*, vol. 45, no. 3, p 534-547, May-June 2008
- <sup>3</sup> Abilleira, Fernando., and Shidner, Jeremy. “Entry, Descent, and Landing Communications for the 2011 Mars Science Laboratory” AIAA Guidance, Navigation, and Control Conference and Co-located Conferences, Minneapolis, Minnesota, August 13-16, 2012.
- <sup>4</sup> Neelon, Joseph, Wallace, Mark, and Craig, Lynn “Coordination of Mars Orbiting Assets to Support Entry, Descent, and Landing (EDL) Activities,” AAS/AIAA Space Flight Mechanics Meeting, Maui Hawaii, February 8-12, 2004
- <sup>5</sup> Premkumar R. Menon, Sean V. Wagner, David C. Jefferson, Eric J. Graat, Kyong J. Lee, William B. Schulze, Robyn M. Woollands and Kevin E. Criddle, “Mars Reconnaissance Orbiter Navigation Strategy for Support of InSight Lander's Entry, Descent and Landing Sequence,” AAS 19-209